

## ARTICLES

## Relativity parameters determined from lunar laser ranging

J. G. Williams, X. X. Newhall, and J. O. Dickey

*Jet Propulsion Laboratory, California Institute of Technology, Pasadena, California 91109*

(Received 5 October 1994; revised manuscript received 14 August 1995)

Analysis of 24 years of lunar laser ranging data is used to test the principle of equivalence, geodetic precession, the PPN parameters  $\beta$  and  $\gamma$ , and  $\dot{G}/G$ . Recent data can be fitted with a rms scatter of 3 cm. (a) Using the Nordtvedt effect to test the principle of equivalence, it is found that the Moon and Earth accelerate alike in the Sun's field. The relative accelerations match to within  $5 \times 10^{-13}$ . This limit, combined with an independent determination of  $\gamma$  from planetary time delay, gives  $\beta$ . Including the uncertainty due to compositional differences, the parameter  $\beta$  differs from unity by no more than 0.0014; and, if the weak equivalence principle is satisfied, the difference is no more than 0.0006. (b) Geodetic precession matches its expected 19.2 marc sec/yr rate within 0.7%. This corresponds to a 1% test of  $\gamma$ . (c) Apart from the Nordtvedt effect,  $\beta$  and  $\gamma$  can be tested from their influence on the lunar orbit. It is argued theoretically that the linear combination  $0.8\beta + 1.4\gamma$  can be tested at the 1% level of accuracy. For solutions using numerically derived partial derivatives, higher sensitivity is found. Both  $\beta$  and  $\gamma$  match the values of general relativity to within 0.005, and the linear combination  $\beta + \gamma$  matches to within 0.003, but caution is advised due to the lack of theoretical understanding of these sensitivities. (d) No evidence for a changing gravitational constant is found, with  $|\dot{G}/G| \leq 8 \times 10^{-12}/\text{yr}$ . There is significant sensitivity to  $\dot{G}/G$  through solar perturbations on the lunar orbit. [S0556-2821(96)01112-5]

PACS number(s): 04.80.Cc, 95.10.Ce

## INTRODUCTION

In July 1969, the Apollo 11 lunar mission placed an array of 100 silica corner-cube laser retroreflectors on the Sea of Tranquillity. Within a few weeks the 2.7 m telescope at the McDonald Observatory on Mt. Locke, Texas, succeeded in detecting photons returned from a laser pulse sent to the reflector. By 1970, the observatory was routinely obtaining ranges with approximate accuracies of 20–30 cm.

Two more reflector arrays were landed by Apollo missions in 1971: one at the crater Fra Mauro and one at Hadley Rille. A French-built reflector aboard the Russian spacecraft Lunakhod II was placed near the crater Le Monnier in early 1973.

These events provided an opportunity for testing relativity, improving the orbit, and measuring effects of interest to geophysics, astronomy, and lunar science. A lunar laser ranging review is given in [1].

The Moon orbits the Earth at a mean distance of 385 000 km. Solar perturbations distort the orbit from an idealized geocentric ellipse at about 1% of that figure. Since the earliest development of the classical theory of gravitation, the lunar orbit has been an important test of that theory. In 1976 lunar ranges of 25 cm accuracy were used to test the strong equivalence principle [2,3], and a decade later the geodetic precession was tested [4,5]. Now that laser range observations to the Moon have accuracies of 3 cm, additional, more stringent tests of relativistic gravitational theory are practical. This paper presents the results of tests of the principle of equivalence, geodetic precession, the parametrized post-Newtonian (PPN) quantities  $\beta$  and  $\gamma$ , and the time rate of change of the gravitational constant  $G$ .

## THE DATA SET

The data set used in this analysis consists of measured round-trip light travel times, here called "ranges," between an observatory and retroreflector. Ranges from three sites cover the time from March 1970 to January 1994. Between 1970 and 1984 the only data used are those from the McDonald Observatory. Then in 1984 two other stations began acquiring ranges: one on Mt. Haleakala on the island of Maui; the other at the CERGA station in Grasse, France. (In 1985 the 2.7 m McDonald instrument ceased laser ranging operation and was replaced by the McDonald Laser Ranging System, a dedicated 60 cm telescope. The Haleakala facility terminated lunar ranging operations in August 1990.)

The lasers currently used in the ranging operate at 10 Hz, with a pulse width of about 200 psec; each pulse contains  $\sim 10^{18}$  photons. Under favorable observing conditions a single reflected photon is detected once every few seconds. For data processing, the ranges represented by the returned photons are statistically combined into normal points, each normal point comprising up to  $\sim 100$  photons. There are 8427 normal points used in this investigation.

The measured round-trip travel times  $\Delta t$  are two way, but in this paper equivalent ranges in length units are  $c\Delta t/2$ . The conversion between time and length (for distance, residuals, and data accuracy) uses 1 nsec = 15 cm. The ranges of the early 1970s had accuracies of approximately 25 cm. By 1976 the accuracies of the ranges had improved to about 15 cm. Accuracies improved further in the mid-1980s; by 1987 they were 4 cm, and the present accuracies are 2–3 cm. One immediate result of lunar ranging was the great improvement

in the accuracy of the lunar ephemeris. Within six years, the fitting of lunar range data reduced the range error from a pre-laser ranging value of approximately 1 km to a few decimeters.

### THE MATHEMATICAL MODEL

The model for the observatory-reflector round-trip time delay includes the geocentric orbit, orientation of the Earth and Moon, tidal displacements of observatory and reflector sites, plate motion, and atmospheric delay. The 3-cm rms postfit range residuals of recent years attest to the success of the models, but it is well to remember that there are always small omitted effects. Some pertinent effects are discussed in later sections. The remainder of this section discusses the relativity modeling.

The simultaneous numerical integration of the Moon and planets uses the solar-system barycenter. This approach establishes the coordinate frame used for the computation of the observable range. Each transmit and receive time at the ranging observatory is transformed to the coordinate time for the solar-system barycenter using the vector formulation of Moyer [6]. Geocentric observatory coordinates and selenocentric reflector coordinates are modified with a Lorentz transformation. The gravity fields of the Sun and Earth delay the signal. Given a transmit time, the computed reflect and receive times are derived from a "light-time iteration."

The formulation of the Jet Propulsion Laboratory (JPL) planetary ephemeris programs is used to estimate the relativity parameters. The principal gravitational force on the nine planets, the Sun, and the Moon is modeled by considering those bodies to be point masses in the isotropic, parametrized post-Newtonian (PPN)  $n$ -body metric [7]. A thorough description of the equations of motion for the planets and Moon is given in [8]. The portion of the model used in relativity analysis is the point-mass acceleration for each of the bodies:

$$\begin{aligned} \ddot{\mathbf{r}}_{i \text{ point mass}} = & \sum_{j \neq i} \frac{\mu_j (\mathbf{r}_j - \mathbf{r}_i)}{r_{ij}^3} \left\{ 1 - \frac{2(\beta + \gamma)}{c^2} \sum_{k \neq i} \frac{\mu_k}{r_{ik}} \right. \\ & - \frac{2\beta - 1}{c^2} \sum_{k \neq j} \frac{\mu_k}{r_{jk}} + \gamma \left( \frac{v_i}{c} \right)^2 + (1 + \gamma) \left( \frac{v_j}{c} \right)^2 \\ & - \frac{2(1 + \gamma)}{c^2} \dot{\mathbf{r}}_i \cdot \dot{\mathbf{r}}_j - \frac{3}{2c^2} \left[ \frac{(\mathbf{r}_i - \mathbf{r}_j) \cdot \dot{\mathbf{r}}_j}{r_{ij}} \right]^2 \\ & + \frac{1}{2c^2} (\mathbf{r}_j - \mathbf{r}_i) \cdot \ddot{\mathbf{r}}_j \left. \right\} + \frac{1}{c^2} \sum_{j \neq i} \frac{\mu_j}{r_{ij}^3} \\ & \times \{ [\mathbf{r}_i - \mathbf{r}_j] \cdot [(2 + 2\gamma)\dot{\mathbf{r}}_i - (1 + 2\gamma)\dot{\mathbf{r}}_j] \} (\dot{\mathbf{r}}_i - \dot{\mathbf{r}}_j) \\ & + \frac{3 + 4\gamma}{2c^2} \sum_{j \neq i} \frac{\mu_j \ddot{\mathbf{r}}_j}{r_{ij}}, \end{aligned} \quad (1)$$

where  $\mathbf{r}_i$ ,  $\dot{\mathbf{r}}_i$ , and  $\ddot{\mathbf{r}}_i$  are the solar-system barycentric position, velocity, and acceleration vectors of body  $i$ ;  $\mu_j = Gm_j$ , where  $G$  is the gravitational constant and  $m_j$  is the mass of body  $j$ ;  $r_{ij} = |\mathbf{r}_j - \mathbf{r}_i|$ ;  $\beta$  is the PPN parameter measuring the nonlinearity in superposition of gravity;  $\gamma$  is the PPN param-

eter measuring space curvature produced by unit rest mass;  $v_i = |\dot{\mathbf{r}}_i|$ ; and  $c$  is the speed of light.

The remaining part of the equations of motion accounts for tides and gravitational harmonics on the Earth and Moon, and the effects of the major asteroids. The lunar rotation is integrated simultaneously with the orbits. Partial derivatives of the orbits and lunar rotation with respect to solution parameters are generated by numerical integration.

The parameter  $\gamma$  also directly affects the measured range. From a geometrical point of view the Sun, Earth, and Moon each curve space in their vicinity to varying degrees. The effect of this curvature is to increase the round-trip travel time of a laser pulse. The complete relativistic light-time expression was derived in heliocentric form by Shapiro [9] in 1964 and independently by Holdridge [10] in 1967. It was formulated in expanded solar-system barycentric form by Moyer [11] in 1977. The portion of Moyer's form due to the Sun and Earth is

$$\begin{aligned} t_j - t_i = & \frac{r_{ij}^B}{c} + \frac{(1 + \gamma)\mu_S}{c^3} \ln \left( \frac{r_i^S + r_j^S + r_{ij}^S + (1 + \gamma)\mu_S/c^2}{r_i^S + r_j^S - r_{ij}^S + (1 + \gamma)\mu_S/c^2} \right) \\ & + \frac{(1 + \gamma)\mu_E}{c^3} \ln \left( \frac{r_i^E + r_j^E + r_{ij}^E}{r_i^E + r_j^E - r_{ij}^E} \right). \end{aligned} \quad (2)$$

The first term on the right is the geometric travel time due to coordinate separation; the remaining two terms represent the curvature effects due to the Sun and Earth. The complete equation gives the elapsed coordinate time between two photon events, where an event is indicated by the subscript  $i$  or  $j$ . Event 1 is transmission, event 2 is reflection, and event 3 is reception. A latin superscript denotes the origin of a vector:  $B$  is the solar-system barycenter,  $S$  is the Sun, and  $E$  is the Earth. In the convention used here, the subscript  $i$  represents the earlier of two photon events,  $j$  the later of the two ( $j = i + 1$ ).

The use of the symbols in the equation is as follows.  $r_i^S = |\mathbf{r}_i^S|$  is the magnitude of the vector from the Sun to photon event  $i$  (transmission or reflection) at coordinate time  $t_i$ ;  $r_j^S$  has the corresponding meaning for photon event  $j$  (reflection or reception).  $r_{ij}^S = |\mathbf{r}_j^S - \mathbf{r}_i^S|$  is the magnitude of the difference between the vector from the Sun to photon event  $j$  at time  $t_j$  and the vector from the Sun to photon event  $i$  at time  $t_i$ .  $\mu_S = GM_{\text{Sun}}$ ;  $\mu_E = GM_{\text{Earth}}$ ; the superscripts  $B$ ,  $S$ , and  $E$  and the parameters  $\gamma$  and  $c$  have the meanings stated above.

When time delay is converted to distance, the dominant effect of space curvature is due to the Sun and averages 7.6 m; the contribution from the Earth is about 4 cm. The ignored effect of the Moon amounts to only 0.6–0.7 mm.

### ANALYSIS

The next four sections give tests of the principle of equivalence, geodetic precession, the PPN quantities  $\beta$  and  $\gamma$ , and the time rate of change of the gravitational constant  $G$ . These least-squares solutions, which use the lunar laser ranging (LLR) data, are separate from one another. The four sections also contain analytical approximations intended to explain how the sensitivities to the foregoing parameters arise. This section discusses analysis procedures common to the four tests.

In the solution process there are approximately 140 estimated parameters besides those connected with relativity, including the lunar orbit, physical librations (rotation), reflector coordinates, elastic deformation (Love numbers), rotational dissipation, moments of inertia, and low-degree gravity field, as well as the mass of the Earth-Moon system, the heliocentric orbit of the Earth-Moon system, Earth station locations, precession and nutation of the equator, and Earth rotation (UT1 and polar motion), and two tidal dissipation parameters. (A secular acceleration of the geocentric lunar longitude arises from the interaction of the Moon with the terrestrial ocean tides.)

Also estimated are the ephemerides of all the planets, the length of the astronomical unit, the Earth-Moon mass ratio, and the masses of selected asteroids [12]. Reliable estimation of the planetary orbits and asteroid masses is achieved by including more than 64 000 planetary observations. Those data do indeed provide a strong determination of the aforementioned parameters, but their presence is not directly used to estimate relativity parameters. This paper is intended as a lunar test of relativity.

Parameter uncertainties derived from least-squares analyses of large data sets are prone to be too small. While random observational errors cause solution parameter uncertainties to improve as the inverse square root of the number of observations, systematic errors need not be so favorable. Systematic errors can be observational or from modeling. They can be too subtle to be apparent when residuals are examined, and, in the case of modeling omissions, the effect may mimic solution parameters. To combat the failure of formal errors, a "realistic" error is constructed in two steps: the standard error from the least-squares procedure is multiplied by a constant factor, and any suspected additional contributions are added in a root-sum-squared fashion.

The parameter errors from the least-squares solution include the effect of individual data weights, postfit rms residuals, data distribution, and correlations between solution parameters. The least-squares solution also includes an error contribution due to Earth rotation. The simultaneous estimation of the planetary parameters contributes uncertainty to the other solution parameters through the lunar orbit. The multiplicative factor comes from experience with (1) changes in solution parameter values due to different data spans and different solutions (marginally determined parameters can be solved for, constrained, or omitted), and (2) solution parameters with independently known values. In this paper, solution parameters given with uncertainties use these scaled errors unless the text indicates otherwise. The results for the equivalence principle and change in  $G$  include additional contributions to the realistic error that are described in those sections.

### THE PRINCIPLE OF EQUIVALENCE

Nordtvedt [13,14] has published an analysis of the effects of a violation of the principle of equivalence. (A consequence of this principle is that the gravitational mass  $M_G$  of any object is identical to its inertial mass  $M_I$ .) The Earth and Moon are accelerated by the gravitational field of the Sun. Failure of the principle of equivalence would cause a differential acceleration between the two bodies, giving a dipole

term in the expansion of the Sun's gravitational field at the Earth. Nordtvedt points out that a failure of the principle would lead to an anomalous radial perturbation with the 29.53-day synodic period between the Moon and Sun. [The synodic period is the reciprocal of the difference between the inverse sidereal periods:  $29.53 = (1/27.32 - 1/365.24)^{-1}$ .] The argument (designated  $D$ ) with the synodic period is the mean longitude of the Moon minus the mean longitude of the Sun and is zero at new moon. Any anomalous radial perturbation will be proportional to  $\cos D$ .

A breakdown of the principle of equivalence gives an acceleration of the Moon with respect to the Earth of  $GM'E\mathbf{r}'/r'^3$ , where  $G$  is the gravitational constant,  $M'$  is the mass of the Sun,  $\mathbf{r}'$  is the vector from the Sun to the Earth-Moon center of mass,  $r'$  is the magnitude of  $\mathbf{r}'$ , and  $E = (M_G/M_I)_{\text{Earth}} - (M_G/M_I)_{\text{Moon}}$  is the difference between the Earth and Moon gravitational-to-inertial mass ratios.

The lunar mean anomaly is  $l$ ; its rate is the natural frequency for radial perturbations. Nordtvedt's first-order expression for a near-circular orbit can be written

$$\Delta r = -a'E \frac{\dot{L}'^2(2\dot{L} + \dot{D})}{\dot{D}(i^2 - \dot{D}^2)} \cos D. \quad (3)$$

In the conventional notation of lunar theory,  $L$  is the mean longitude of the Moon,  $L'$  is the mean longitude of the Sun ( $180^\circ$  from the heliocentric mean longitude of the Earth-Moon barycenter),  $a'$  is the heliocentric semimajor axis of the Earth-Moon barycenter orbit, and  $D = L - L'$ . (Overdots indicate rates; primes denote quantities referring to the Sun.)

As a check of Nordtvedt's original result, a somewhat different derivation based on perturbations of orbital elements was performed. It gives

$$\Delta r = -a'E \frac{i\dot{L}'^2(2i + \dot{D})}{\dot{L}\dot{D}(i^2 - \dot{D}^2)} \cos D. \quad (4)$$

When evaluated in meters, the two coefficients are  $-2.08 \times 10^{10}E$  and  $-2.05 \times 10^{10}E$ , respectively. The difference between the two is only 1.4%. It will be noted that the denominator contains the combination  $i - \dot{D}$ , which is the difference between the solar mean motion and the lunar perigee precession  $\dot{L}' - \dot{\omega}$ . A breakdown of the equivalence principle would also give rise to a perturbation in longitude proportional to  $\sin D$ . For  $a\Delta L$ , where  $a$  is the semimajor axis of the lunar orbit, the companion to Eq. (4) has a coefficient  $-2.1$  times larger.

Recently Nordtvedt [15] has demonstrated that the earlier-derived coefficients of  $\cos D$  need to be increased by about 40% over the values given above; this increase is supported by Damour and Vokrouhlický [16]. This amplification arises because of the strong solar influence on the lunar orbit. The synodic period of the perturbation interacts with the  $2D$  tidal expansion of the solar field at the Earth. With this correction the radial perturbation in meters is

$$\Delta r = -2.87 \times 10^{10}E \cos D. \quad (5)$$

The longitude perturbation also needs to be increased by about 40%.

The above equations apply to any violation of the principle of equivalence. A breakdown of the strong equivalence principle, where gravitational self-energy  $U_G$  can influence the gravitational interaction, is possible for bodies the size of the Earth and Moon. Nordtvedt gives

$$\frac{M_G}{M_I} - 1 = \eta \frac{U_G}{Mc^2}. \quad (6)$$

The quantity  $\eta$  depends on the PPN parameters  $\beta$  and  $\gamma$  according to

$$\eta = 4\beta - \gamma - 3 \quad (7)$$

and is zero for general relativity. Numerically, the difference between the Earth and Moon is

$$E = (-4.64 \times 10^{-10} + 0.19 \times 10^{-10}) \eta = -4.45 \times 10^{-10} \eta. \quad (8)$$

Expressed in terms of  $\eta$ , the radial perturbation in meters is  $\Delta r = 12.8 \eta \cos D$ . The coefficients in [16] are 2% larger than in [15], so the coefficient of the last expression is  $13.1 \eta$ , and the coefficient in Eq. (5) is  $-2.94 \times 10^{10} E$ .

The numerical values in Eq. (8) are the same as used in [2], where the Earth's self-energy is based on the result [17] for a structured interior, and the Moon's self-energy is based on a homogeneous interior. Our own computation for the self-energies for radially structured interiors for both bodies recovered the earlier values to the number of digits given in Eq. (8). Adelberger *et al.* [18] have suggested a 10% larger value for the Earth, but a recent computation is in agreement with Eq. (8) [19].

Apart from the Nordtvedt effect, there are other causes of  $\cos D$  signatures in the lunar distance. From the classical expansion of the lunar orbit [20] there is a  $(109 \text{ km}) \times \cos D$  term in the radial coordinate. The amplitude depends on mass ratios, mean motions, and the mean distance to the Moon, but these are well enough known that only 2 mm error occurs for this coefficient (the least-squares solution for the equivalence principle includes this error). There is also a relativistic contribution apart from the Nordtvedt effect which has been computed in [15,21–26]. This relativistic contribution is given as  $-(6 \text{ cm}) \times \cos D$  in [23]. The numerical integration of the relativistic equations of motion include classical and relativistic orbit signatures in our lunar ephemeris. Williams *et al.* [2] mention that the interaction between the Earth's gravitational second harmonic  $J_2$  and the Sun gives rise to a  $-(5 \text{ cm}) \times \cos D$  effect ( $-7 \text{ cm}$  with the 40% increase). This force is included in our equations of motion.

The former effects are modeled in our programs, but solar radiation pressure gives rise to a small unmodeled signature [15,27]. This effect is estimated to be  $-(0.35 \text{ cm}) \times \cos D$ . The numerical integration software contains a model for the solar gravity field but not for solar radiation pressure. In the range computation the differences between the transmit, reflect, and receive times are computed by iteration, and the time delay of Eq. (2) is modeled, implying that there should be no anomalous signatures due to these sources [28].

The equivalence principle is tested by fitting LLR data with a least-squares solution. The partial derivative for  $M_G/M_I$  is generated by numerical integration (prior to the

results in [5] we used the  $\cos D$  formulation). The result is  $E = (4.3 \pm 4.6) \times 10^{-13}$ . This is equivalent to  $-1.2 \pm 1.3 \text{ cm}$  in the coefficient of  $\cos D$  or, for a violation of the strong equivalence principle, to  $\eta = -0.0010 \pm 0.0010$ . The argument  $D$  is unevenly sampled. Ranges are never acquired near new Moon because of the bright Sun. The former 2.7 m McDonald Observatory ranging system could acquire ranges near full Moon, but the newer, more accurate, lower-energy-per-pulse systems have acquired full-Moon ranges only during an eclipse. Wishing to be cautious about uncertainties, we have used the procedure of [1]. In a root-sum-squared sense, 1 cm has been included in the above uncertainty in the coefficient of  $\cos D$ ,  $3.5 \times 10^{-13}$  in  $E$ , and 0.0008 in  $\eta$ . If the unmodeled 0.3 cm effect from solar radiation pressure is applied as a correction, then  $E = (3.2 \pm 4.6) \times 10^{-13}$ , the  $\cos D$  coefficient is  $-0.9 \pm 1.3 \text{ cm}$ , and  $\eta = -0.0007 \pm 0.0010$ . In the solution for  $E$ , the largest correlations of 0.4 occur with  $GM_{\text{Earth+Moon}}$ , lunar semimajor axis  $a$ , and eccentricity  $e$ . These occur because a  $\cos 2D$  term is important for the  $GM$  determination and will not be independent of the  $\cos D$  term because of nonuniform sampling, and because of the facts that the semimajor axis is connected to  $GM$  through Kepler's third law and that the product  $ae$  is better determined than  $e$ .

The LLR results for  $E$  and the  $\cos D$  coefficient apply to the equivalence principle, weak or strong:  $E_{\text{LLR}} = E_{\text{SEP}} + E_{\text{WEP}}$ . Earlier results for the Nordtvedt effect have been interpreted in terms of the strong equivalence principle, the laboratory results for the weak equivalence principle being able to rule out effects due to composition. Limits as low as those given above require consideration of the weak equivalence principle [24]. Adelberger *et al.* [18,29] have combined their Eötvös results with the Princeton [30] and Moscow [31] Eötvös experiments. For acceleration in the solar field they place limits on the fractional acceleration due to composition. Su *et al.* [32] have used test bodies which simulate the compositional differences of the Earth and Moon. Their compositional contribution  $E_{\text{WEP}}$  is  $(-1.6 \pm 2.2) \times 10^{-12}$ . When combined with the LLR value,  $E_{\text{SEP}} = (1.9 \pm 2.3) \times 10^{-12}$ . Note that the Nordtvedt test is a null result. It would be necessary to have compensating violations of the strong and weak equivalence principles to simultaneously satisfy the small LLR observational uncertainties in  $E$  while using a larger uncertainty from the weak equivalence principle.

We wish to derive  $\beta$  from  $\eta$  and  $\gamma$  using  $\beta = (\eta + \gamma + 3)/4$ . The uncertainty for  $\gamma$  is taken to be 0.002 from the interplanetary time delay [33]. The compositional constraints from the preceding discussion contribute to  $\eta$  and  $\beta$ . Using  $E_{\text{SEP}}$  from the combined compositional [32] and LLR results gives  $\eta = -0.0043 \pm 0.0051$ . With the combined strong and weak equivalence principles,  $\beta = 0.9989 \pm 0.0014$ . Under the assumption that the weak equivalence principle is satisfied,  $\beta = 0.9998 \pm 0.0006$ .

Previously reported results for the Nordtvedt effect are given in [1–3,5,34–37]. The uncertainty in determinations of the Nordtvedt effect has decreased by a factor of 30 during 18 years. The results given in [1] and [37] have uncertainties comparable to those in this paper.

### GEODETIC PRECESSION

The geodetic precession is also called both the geodesic precession and the de Sitter–Fokker precession. It contributes a 19.2 marc sec/yr precession rate for a gyroscope moving with the Earth. For an elliptical orbit about the Earth, the same contribution is made to the precession of the node and of the longitude of perigee along the ecliptic. The geodetic precession rate is prograde and is computed from [38] and [39] to be

$$P_g = (1/2 + \gamma) \frac{(n' a'/c)^2 n'}{1 - e'^2} \quad (9)$$

where  $c$  is the speed of light and, for the orbit of the Earth–Moon system about the Sun,  $n'$  is the mean motion,  $a'$  the semimajor axis, and  $e'$  the eccentricity.

We review and extend the discussion of [40], which proposes testing for the geodetic precession using LLR data. The distance from the center of the Earth to the center of the Moon can be represented by the series [20] with largest terms (in kilometers)

$$r = 385\,001 - 20\,905 \cos l - 3699 \cos(2D - l) - 2956 \cos 2D + \dots \quad (10)$$

The first term is the mean distance, the second results from the eccentricity of the orbit, and the third and fourth are from solar perturbations. The lunar mean anomaly is  $l$  (27.56-day period), and  $D$  is the mean elongation of the Moon from the Sun (29.53-day period).

For purposes of explanation, we can imagine that the least-squares solutions are equivalent to determining amplitudes, phases, and phase rates of individual terms in Eq. (10). More exactly, there are a limited number of free parameters in a solution, so that the amplitudes, phases, and phase rates are not all independent. The amplitude of a well sampled frequency can be reliably measured to 1 cm. From the second term one expects to determine the mean anomaly to 0.1 marc sec and the anomalistic mean motion  $\dot{l}$  with correspondingly high accuracy. Limitations, which increase the uncertainty, include the need to also determine quadratic ( $t^2$ ) and long-period (18.6-yr period of the node) tidal contributions to the mean anomaly [41], terms at nearby frequencies which require 6.0-year (period of the argument of perigee) and 8.9-year (period of the longitude of perigee) data spans to separate fully, and a span of the most accurate data, which is 7 yr long. From the two solar perturbation terms and the mean anomaly, one gets  $D$  with sub-marc sec accuracy and its rate with corresponding accuracy. It is presumed that the planetary data give  $\dot{L}'$ . Since  $D = L - L' = \bar{\omega} + l - L'$ , the rate of the longitude of perigee,  $\bar{\omega}$ , is determined. The geodetic precession can be thought of as being detected through its influence on the lunar longitude-of-perigee precession rate. In addition to the errors in  $l$  and  $\dot{L}'$ , we must ask what errors are present in the longitude-of-perigee rate.

The lunar perigee precession rate is dominated by solar perturbations. While the classical contributions to the perigee precession rate from lunar and solar orbital parameters are mostly very well known, two influences merit discussion. An error in the inclination of the lunar orbit plane to the ecliptic

plane of 1 marc sec would introduce a 0.18 marc sec/yr uncertainty in the perigee precession rate. The orientation of the planes of the lunar orbit, ecliptic, and the Earth's equator are determined by the LLR data; it takes 18.6 yr to get a full separation of these parameters. Thus the uncertainty in the lunar inclination has been decreasing strongly with time, and a good test of the geodetic precession is a benefit of the long data arc. The error in the first LLR tests of geodetic precession [4,5] was dominated by the inclination uncertainty. Because the highest-quality data extend over only the past seven years, the uncertainty of the inclination should continue to improve in the future. When geodetic precession is fixed at the value of general relativity, the inclination uncertainty is 0.5 marc sec, contributing 0.09 marc sec/yr to precession uncertainty; when geodetic precession is estimated, the inclination uncertainty is 0.7 marc sec, contributing 0.12 marc sec/yr. This source of error should continue to decrease with increasing data span.

The second significant source of perigee precession error comes from the lunar second-degree gravitational harmonics  $J_2$  and  $C_{22}$ . Since the ratio is accurately known from the LLR analyses, we will refer to the error in  $J_2$  only. Until recently we have used a 0.6% uncertainty for the lunar  $J_2$ , corresponding to a precession error of 0.11 marc sec/yr (0.6% of the geodetic precession). This  $J_2$  uncertainty came from [35], which combined the analysis of Lunar Orbiter Doppler data and LLR data in a single solution. It was the Lunar Orbiter data which determined the  $J_2$  in that combination. There have been three recent developments: LLR now determines the second-degree lunar harmonics [1] as accurately as the earlier Lunar Orbiter analysis, the Lunar Orbiter data have been extensively reanalyzed [42] with an improvement in accuracy, and newer Clementine mission data have been analyzed [43]. The three recent results are concordant [44]. As we now include the lunar  $J_2$  as a solution parameter, the  $J_2$  uncertainty, like the inclination error, is accounted for during the least-squares solutions.

The equations of motion for the numerical integration of the lunar and planetary ephemerides in Eq. (1) are those of general relativity. They contain the inherent geodetic precession effects.

Geodetic precession is implicit in the relativistic equations of motion [Eq. (1)]. An explicit development is needed for the partial derivative. We isolated the terms which give rise to the geodetic precession by selecting torquelike terms that cause the node to precess. The leading terms in (Moon distance)/(Sun distance)  $\approx 1/400$  were retained. A scale factor  $K_{GP}$  represents a possible departure from the prediction of general relativity:

$$\ddot{\mathbf{r}}_M - \ddot{\mathbf{r}}_E = K_{GP} \frac{2\mu_S}{c^2 r_B^3} \{ -\gamma [\dot{\mathbf{r}}_B \cdot (\dot{\mathbf{r}}_M - \dot{\mathbf{r}}_E)] \mathbf{r}_B + (1 + \gamma) [\mathbf{r}_B \cdot (\dot{\mathbf{r}}_M - \dot{\mathbf{r}}_E)] \dot{\mathbf{r}}_B \} \quad (11)$$

where the quantities  $\mathbf{r}_E$ ,  $\mathbf{r}_M$ , and  $\mathbf{r}_B$  denote the solar-system barycentric positions of the Earth, Moon, and Earth–Moon barycenter, respectively, and time is referenced to the solar-system barycenter. In the solutions a null value of  $K_{GP}$  corresponds to general relativity.

By using perturbation theory with an elliptical orbit, it was verified for a unit of increment of  $K_{GP}$  that Eq. (11) gives the precession rate of Eq. (9) for the node and longitude of perigee. Nordtvedt [45] has pointed out that Eq. (11) can be split into symmetric and antisymmetric parts. The antisymmetric part influences the precession of a gyroscope or an elliptical orbit, but there is a contribution to the precession of the perturbed lunar orbit from the symmetric part. The latter contributions to the precessions of the node and of the longitude of perigee need not be equal, and they do not depend on  $\gamma$ . The LLR test is similar, though not identical, to the test on a precessing gyroscope.

Using LLR data, the solution for the geodetic precession correction is

$$K_{GP} = -0.003 \pm 0.007. \quad (12)$$

The largest correlation of +0.56 is with the lunar  $J_2$ ; this parameter is now at least as important an error source as the orbit inclination. Equation (9) does not give the precession identical to that of Eq. (11) with unit increment for  $K_{GP}$ , but we note that the total relativistic precession from Eq. (1) is within 10% of Eq. (9) [15,21–23]. Consequently, we approximate  $\sigma(\gamma) \approx \frac{3}{2}\sigma(K_{GP})$  and conclude that the above result for  $K_{GP}$  corresponds to a 1% test of  $\gamma$ , implying a precession rate error of 0.13 marc sec/yr.

Bertotti *et al.* [40] did not fit data but argued that geodetic precession was being satisfied (a) from the small size of the LLR residuals, and (b) from the agreement between LLR and VLBI Earth rotation rates. Direct fits to the LLR data [4,5] confirmed geodetic precession to 2%. More recently, Dickey *et al.* [1] give a 0.9% test. The result above reduces the uncertainty to 0.7%. All results are consistent with  $\gamma=1$  and general relativity.

### THE PPN PARAMETERS

The PPN parameters of interest are  $\beta$ , measuring the non-linearity in the superposition of gravity, and  $\gamma$ , measuring the amount of space curvature produced by unit rest mass. In general relativity both parameters are unity. Estimates of  $\gamma$  and  $\beta$  have been obtained by other investigators. Shapiro *et al.* [46], Cain *et al.* [47], and Hellings [48] used the Viking orbiter and lander data to determine  $\gamma$ . Reasenberg *et al.* [33] estimate the uncertainty in  $\gamma$  to be 0.002, using Viking lander data. The test of the geodetic precession in the preceding section can be taken as a 1% test of  $\gamma$ , but this statement ignores additional sensitivity to PPN parameters, discussed below.

The lack of detection of Nordtvedt's term has been used earlier to imply a small uncertainty (0.0014) on  $\beta$ . Tests of  $\beta$  using the planetary range data [36] yield a  $\beta$  uncertainty of 0.003. There is value in attempting to test  $\beta$  and  $\gamma$  in an alternative manner.

Distinct from the Nordtvedt term, the relativistic point-mass interactions of Eq. (1) give sensitivity of the lunar orbit to  $\beta$  and  $\gamma$ . Partial derivatives for  $\beta$  and  $\gamma$  have been generated from Eq. (1) by numerical integration. The orbit perturbations include the geodetic precession. Thus one expects solutions for  $\gamma$  to have uncertainties comparable to, or better than, the above 1% test resulting from the geodetic precession.

LLR solutions for  $\beta$  and  $\gamma$  using the sensitivity from the relativistic point-mass interactions and the gravitational time delay Eq. (2), but not the Nordtvedt term, show a smaller uncertainty for  $\gamma$  than would be predicted from the geodetic precession alone, and nearly identical accuracies for both  $\beta$  and  $\gamma$ . When  $\beta$  and  $\gamma$  are estimated simultaneously, we find that both uncertainties are 0.005, there are no significant deviations from 1, and the  $-0.86$  correlation between  $\beta$  and  $\gamma$  means that the linear combination  $\beta + \gamma$  is better determined, with an uncertainty of 0.003. The challenge is to understand the source of this sensitivity and whether it is valid.

The discussion of the geodetic precession presented the view that the sensitivity to that precession comes from the solar perturbations in combination with the elliptical radial variations. In that discussion, the determination of the rate of the angle  $D = L - L' = \bar{\omega} + l - L'$  was presented as giving sensitivity to the geodetic precession, and hence  $\gamma$ , through the lunar perigee rate. When the relativistic point-mass interactions are considered, the rate of  $D$  also gives sensitivity to  $\beta$  and  $\gamma$  as they influence  $\dot{L}'$ . In the near circular approximation, the angular rate of the Earth-Moon system about the Sun is given by an expression resembling Kepler's third law (e.g., see [15,21,49]):

$$\dot{L}' = [(GM')^{1/2}/A'^{3/2}][1 - S(\beta + \gamma/2)]. \quad (13)$$

$A'$  is the unperturbed semimajor axis  $a'$  plus the change in the mean distance from the Sun when relativistic perturbations are included,  $G$  is the gravitational constant, and  $M'$  is the solar mass ( $GM' = n'^2 a'^3$ ). The scale for relativistic effects is set by

$$S = GM'/a'c^2 = (n'a'/c)^2 = 0.98706 \times 10^{-8} \quad (14)$$

with  $Sa' = 1.4766$  km and  $Sn' = 12.792$  marc sec/yr. The relativistic contribution to the angular rate is  $-Sn'(\beta + \gamma/2)$ . The relativistic contribution to  $\dot{\omega} - \dot{L}'$  is then  $Sn'(0.5 + \beta + 1.5\gamma)$  when the geodetic precession is included, but is closer to  $Sn'(0.65 + 0.8\beta + 1.4\gamma)$  when a more exact expression for the perigee rate is included [15,21,22]. From the experience with the geodetic precession, the linear combination of  $\beta$  and  $\gamma$  should be determinable to 1%. This argument assumes that the lunar mean anomaly rate is well determined by the LLR data and that the mean distance from the Sun and  $GM'$  (equivalent to the length of the astronomical unit) are well determined by the planetary range data.

The solutions include both the LLR and planetary ranging data. A normal set of solution parameters is used for the initial conditions of the Moon and planets, but the relativity solution parameters were "turned on" only for the LLR data. Both data sets are sensitive to the heliocentric Earth-Moon orbit. In an attempt to isolate the relativistic sensitivities of the LLR data from those of the planetary data, a double standard is being applied to the heliocentric orbit. The planetary data are included so that appropriate uncertainties in the heliocentric orbit will be propagated into the lunar orbit during the solutions. The double standard is not perfect, but we do not see another way to isolate the contributions of the lunar data from the planetary data. We have done a variety of solutions (see below), including those with planetary relativity parameters turned on, and they do support strong sensitivity of the LLR data to relativity.

The solution cannot be finding all of its  $\beta$  and  $\gamma$  sensitivity through the argument  $D$ , or the two parameters would not separate. Other terms with smaller amplitudes give less sensitivity to other arguments; for example, sensitivity to the mean anomaly  $l'$  of the orbit about the Sun is an order of magnitude less than the mean longitude sensitivity. Sensitivity through the amplitudes is a possibility. Brumberg and Ivanova [21,22] and Nordtvedt [15] have investigated the sensitivities of the amplitudes to  $\beta$  and  $\gamma$ . When one considers observable amplitudes, the  $\beta$  and  $\gamma$  sensitivities are mostly at the few-centimeter level. Brumberg and Ivanova show two notable possibilities. The annual  $\cos l'$  term shows a  $(-16+26\beta-6\gamma)$ -cm relativistic contribution to its amplitude, and the  $\cos D$  term has  $(33-48\beta+10\gamma)$  cm in its amplitude. Nordtvedt does not compute the former term; for the latter term he gets a similar-sized sensitivity. For general relativity ( $\beta=\gamma=1$ ), the Brumberg and Ivanova solution can also be compared to the solution by Lestrade and Chapront-Touzé [23]. The agreement is good except for a few terms involving the annual argument  $l'$ ; this difference seems to be traceable to the 1.66-msec annual term in the time transformation between the solar-system barycenter and the Earth-Moon barycenter. A 1-cm sensitivity to both amplitudes would give a 1.8% uncertainty for  $\beta-0.2\gamma$ . In combination with a 1% determination of  $0.8\beta+1.4\gamma$  from the argument rate for  $D$ , the  $\beta$  uncertainty would be 1.6%, and the  $\gamma$  uncertainty 1.1%. These uncertainties are three and two times, respectively, the uncertainties from the least-squares solution using the LLR data.

In an attempt to better understand the small uncertainties from the least-squares solutions for  $\beta$  and  $\gamma$ , several additional least-squares solutions were done with the following results. (1) If  $\gamma$  is the only relativity parameter in the solution, the resulting uncertainty is 25% of that predicted from the  $K_{GP}$  uncertainty using Eq. (9). (2) If  $\gamma$  and  $K_{GP}$  are simultaneously solved for, the correlation is  $-0.34$ , and both uncertainties are only 1.06 times larger than those from the two individual solutions. (3) The influence of  $\dot{L}'$  [Eq. (13)] in the  $D$  argument rate was weakened by allowing the planetary data to solve for a  $\beta$  and  $\gamma$  pair that differed from the  $\beta$  and  $\gamma$  pair from the lunar data. Compared to a solution for the latter two parameters, the uncertainty in the mean motion about the Sun increased by a factor of 1.55 while the lunar-determined uncertainties for  $\beta$  and  $\gamma$  increased by factors of 1.01 and 1.14, respectively. All least-squares solutions support smaller uncertainties for  $\beta$  and  $\gamma$  than is accounted for by our simplified analytical approximations. The complexity of the perturbed lunar orbit has resisted simplification.

Concerning the sensitivity of the LLR data to  $\beta$  and  $\gamma$  through point-mass interactions, theory indicates it should be possible to determine the combination  $(0.8\beta+1.4\gamma)$  to 1% uncertainty through an argument rate. There is additional sensitivity to  $\beta$  and  $\gamma$  through amplitudes. Solutions with LLR data give  $\beta$  and  $\gamma$  uncertainties of 0.5%, several times better than our theoretical understanding supports. It is clearly worthwhile to combine the relativistic solutions from both the LLR and planetary ranging data. Since the LLR data have their sensitivity through the lunar and heliocentric orbit, while the planetary data have their main sensitivity to  $\gamma$  through the time delay in the solar gravity field and their main sensitivity to  $\beta$  through the precession of Mercury's

perihelion, the combination of data types offers an interesting possibility. A combined solution would improve the accuracy of separating  $\beta$  and the solar  $J_2$ , which do not separate well when using the existing planetary data alone.

#### CHANGE IN THE GRAVITATIONAL CONSTANT

Analyses of the LLR data have the potential to determine the rate of change of the gravitational constant  $G$ . A decreasing  $G$  would cause both the lunar mean distance and period to increase (from Kepler's third law, the change in mean motion  $n$  and semimajor axis  $a$  are connected:  $2\dot{n}/n+3\dot{a}/a=\dot{G}/G$ ). Tidal dissipation also causes the mean distance and orbital period to increase (for tidal changes,  $2\dot{n}/n+3\dot{a}/a=0$ ), but not in the same ratio as for  $\dot{G}$ . Since the tidal effect is relatively large ( $\dot{n}/n=-1.5\times 10^{-10}/\text{yr}$ ,  $\dot{a}/a=1.0\times 10^{-10}/\text{yr}$ ), and since we are interested in  $\dot{G}/G$  less than  $10^{-11}/\text{yr}$ , accurate tidal modeling is a necessity.

Tides on the Earth dissipate energy and transfer angular momentum from the Earth's spin to the lunar orbit. Our present tidal model includes dissipation by diurnal and semidiurnal tides on the Earth as well as dissipation in the Moon. From a recent solution without  $\dot{G}$  [1] these contribute to the total tidal  $\dot{n}$  or  $\dot{a}$  in the proportions 16%, 86%, and  $-1.5\%$ , respectively. The uncertainty in that total is 2%. The diurnal and semidiurnal terms are separable by a small 18.6-yr term in mean anomaly [41]. The dissipation in the Moon is mainly observed through its influence on the lunar rotation and not on the orbit. The influence on the orbit is inferred from the lunar dissipation model. There are two possible sources of dissipation in the Moon: solid-body tidal dissipation, and viscous or turbulent dissipation at a liquid-core-solid-mantle interface [50]. The former source is programmed in our software; the latter is not. The two sources do not give rise to the same orbital effects, so the lunar contribution may be in error by most of its present 1.5% effect (the larger of the two possibilities) corresponding to  $1\times 10^{-12}/\text{yr}$  in  $\dot{G}/G$ . It is expected that changes in the lunar model would leave the total tidal  $\dot{n}$  and  $\dot{a}$  the same, so the present tidal model should be capable of supporting tests for  $\dot{G}/G$  with the accuracies of this paper. Programming the alternative lunar dissipation model would broaden the tidal acceleration computation, might improve the fit, and should benefit future tests.

A  $\dot{G}/G$  rate of  $-10^{-11}/\text{yr}$  causes a 3.9 mm/yr increase in the lunar mean distance ( $\dot{a}/a=-\dot{G}/G$ ,  $\dot{n}/n=2\dot{G}/G$ ). More important than the linear increase in distance, both  $\dot{G}$  and tidal acceleration contribute a  $-t^2 \sin l$  signature in range that comes from the  $-t^2$  change in mean anomaly. However, even if the  $t^2$  term in mean anomaly were indistinguishable for  $\dot{G}$  and tidal acceleration, the change in mean distance would still be distinct for the two effects. Above, relations between  $\dot{n}$  and  $\dot{a}$  were given for tidal dissipation and  $\dot{G}$ . If  $\dot{G}$  were hidden as a false tidal acceleration with identical  $\dot{n}$ , the difference  $(\dot{a}-\dot{a}_{\text{false tidal}})/a=\dot{G}/3G$ , so that  $-1/3$  of the radial change, or  $-1.3$  mm/yr, would be distinct from tidal acceleration. A change in  $G$  also causes accelerations in the angular motion about the Sun ( $\dot{n}'/n'=2\dot{G}/G$ ), and the solar perturbation terms in Eq. (10) contribute additional sensitivity (the part distinct from tides in  $\ddot{D}$ , the acceleration of the mean longitude of the Moon minus that of the Sun, is

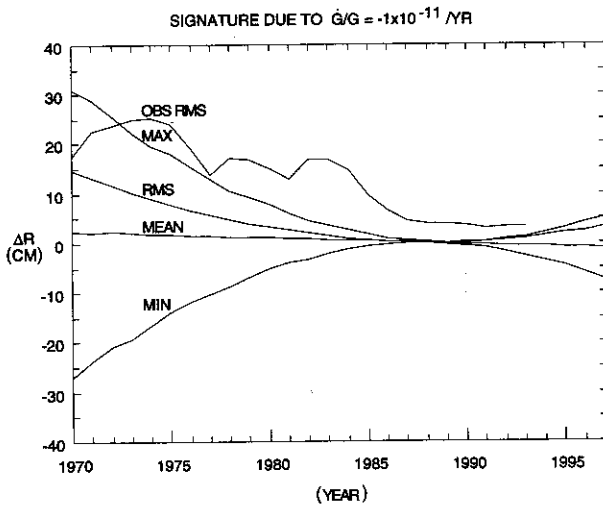


FIG. 1. Effect of  $\dot{G}/G = -1 \times 10^{-11}/\text{yr}$  on the radial coordinate of the Moon. The curves are annual samples of the observed weighted rms range residual and four curves based on the theoretical signature: the maximum, rms, average, and minimum. (The order is the same for the earliest and latest times.) The reference time in Eq. (16) is 1989.

$-2n' \dot{G}/G$ ). The contribution from the acceleration in the heliocentric orbit through the solar perturbation terms gives coefficients of periodic terms which are quadratic in time. With the linear and solar perturbation terms, the  $\dot{G}$  contribution to radial distance that is distinct from tidal acceleration is

$$\frac{1}{3} r \frac{\dot{G}}{G} t - 2n' \frac{\dot{G}}{G} [3699 \sin 2D + 2956 \sin(2D-l) + \dots] t^2 \text{ km.} \quad (15)$$

Some small terms from the sensitivity of the coefficients of the periodic terms to mean-motion changes have been ignored.

For a  $\dot{G}/G$  rate of  $-10^{-11}/\text{yr}$ , the major radial terms are

$$-1.28t + [0.46 \sin(2D-l) + 0.37 \sin 2D] t^2 \text{ mm,} \quad (16)$$

with  $t$  in years. For data spans of more than a decade, the nonlinear terms surpass the linear term in importance. The envelope, rms, and average signature due to Eq. (16) are shown in Fig. 1, along with the annual weighted postfit rms LLR residuals. A rate of  $10^{-11}/\text{yr}$  would yield signatures from the solar perturbations exceeding 10 cm rms ( $>20$  cm extremum) in the early 1970s and reaching 1.0 cm rms (2.6 cm extremum) in 1993; the lack of such signatures demonstrates the importance of the early data in conjunction with the later, more accurate data in limiting  $\dot{G}$ . An increasing data span has the potential to strikingly improve the  $\dot{G}/G$  determination.

The LLR data have been used to estimate  $\dot{G}/G = (1 \pm 3) \times 10^{-12}/\text{yr}$ . Tidal and other standard Newtonian parameters were included in the solution. The largest correlation is  $+0.67$  and is with the semidiurnal tidal component. A more cautious uncertainty will be used. Earlier in this paper a 1-cm sinusoidal signature, 0.7 cm rms, is used for a securely detectable signature. The value 0.7 cm rms in 1993

TABLE I. Four solutions for relativity parameters.

Solution	Parameter	Value
1. Equivalence principle	$E$	$(3.2 \pm 4.6) \times 10^{-13}$
2. Geodetic precession	$K_{GP}$	$-0.003 \pm 0.007$
3. PPN superposition and curvature	$\beta$	$1.003 \pm 0.005$
	$\gamma$	$1.000 \pm 0.005$
4. Change in $G$	$\dot{G}/G$	$(1 \pm 8) \times 10^{-12}/\text{yr}$

justifies a  $\dot{G}/G$  uncertainty of  $7 \times 10^{-12}/\text{yr}$ . Combining with the least-squares result, which adds some tidal uncertainty, the LLR  $\dot{G}/G$  result is  $(1 \pm 8) \times 10^{-12}/\text{yr}$ .

As a check of the linear effect in Eq. (15), a separate solution has estimated a rate in the mean distance along with tidal and other standard solution parameters, but not  $\dot{G}$ . The mean distance rate uncertainty is 3.5 mm/yr, equivalent to  $2.7 \times 10^{-11}/\text{yr}$  for  $\dot{G}/G$ . The previous solution implies a smaller  $\dot{G}/G$  uncertainty, illustrating the dominance of the nonlinear solar perturbation terms.

The present LLR results for  $\dot{G}/G$  do not improve significantly on the planetary ranging results [36,51–53]. Recent results have also been given for planetary data combined with LLR data [54] and the binary pulsar [55–58].

## CONCLUSIONS

Solutions using 24 years of lunar laser data have been used for three tests of relativity and a check of the invariance of the gravitational constant. The results of the four tests are summarized in Table I. The LLR data have improved with time. The data since 1987 are particularly accurate, with 1987 ranges showing a weighted rms residual of 4 cm and 1993 residuals scattering by 3 cm.

The Nordtvedt effect gives strong sensitivity to any violation of the equivalence principle. By using a numerically derived partial derivative for the gravitational-to-inertial mass ratio, we find that  $|(M_G/M_I)_{\text{Earth}} - (M_G/M_I)_{\text{Moon}}| \leq 5 \times 10^{-13}$ . Since any violation of the strong equivalence principle depends on  $\beta$  and  $\gamma$ , and since there are good determinations of  $\gamma$  from interplanetary time-delay measurements, then including the uncertainty due to compositional differences between the Earth and Moon gives  $|\beta - 1| \leq 0.0014$ . If it is assumed that the weak equivalence principle is satisfied, then  $|\beta - 1| \leq 0.0006$ .

The geodetic precession is within 0.7% of its expected value of 19.2 marc sec/yr. Since this precession depends on  $\gamma$ , this result is also a 1% test of  $\gamma$  under the assumption that other relativistic effects are known. The lunar  $J_2$  and the orbit inclination are the most important sources of uncertainty.

Independent of the Nordtvedt effect, but including the geodetic precession, there are orbit perturbations depending on  $\beta$  and  $\gamma$ . The time delay gives some sensitivity to  $\gamma$ . The LLR solutions use numerically derived partial derivatives for the orbit perturbations and indicate sensitivity to  $\beta$  and  $\gamma$  beyond that expected from theoretical work. It is certain that the linear combination  $0.8\beta + 1.4\gamma$  is tested at the 1% level since it arises through the same solar perturbation terms which give the geodetic precession test. The work of Brumberg and Ivanova indicates additional sensitivity to  $\beta$  and  $\gamma$



through annual and synodic monthly terms, and Nordtvedt's work supports sensitivity in the latter term. Neither work would support  $\beta$  and  $\gamma$  uncertainty better than 1%. From the LLR solutions  $\beta$  and  $\gamma$  match the values of general relativity within the uncertainty of 0.005, and the linear combination  $\beta + \gamma$  matches within 0.003. For the LLR solutions it must be cautioned that use is made of the planetary ranging data to determine the distance of the Earth-Moon orbit from the Sun, without allowing those data to directly contribute to the determination of the PPN parameters. It is important to understand this test better, since the sensitivity to  $4\beta - \gamma$  from the Nordtvedt effect in combination with the sensitivity to  $\beta + \gamma$  gives a test of  $\gamma$  with uncertainty 0.003, which is second in accuracy only to the interplanetary time delay, and it can be expected to improve in the future.

On the question of a changing gravitational constant, solutions show no significant change, with  $|\dot{G}/G| \leq 8 \times 10^{-12}/\text{yr}$ . It previously has been understood that  $\dot{G}$  and tidal acceleration both influence the lunar period and mean distance, but  $\dot{G}$  and tidal acceleration would be separable from a linear term in time for distance. Here it is shown that the influence of  $\dot{G}$  also causes nonlinear time signatures, through the solar perturbations, which are already dominant with the present data span.

The lunar orbit is highly perturbed by the Sun. This paper's tests of relativity and  $\dot{G}$  all depend on the solar perturbations. Reasoning from two-body theory is insufficient for the lunar orbit. All of the tests will improve with additional

data of present quality. The geodetic precession test, depending on a secular effect, will benefit from increased data span. The tests of  $\beta$  and  $\gamma$  through orbit perturbations (apart from the Nordtvedt effect) are the least well understood, but hold promise. In combination, the lunar and planetary ranging data should be able to improve on the dynamical determination of the solar  $J_2$ . Finally, there are lunar  $\dot{G}$  terms, nonlinear in time, which should permit significant future improvements in testing the invariance of  $G$ .

#### ACKNOWLEDGMENTS

Helpful comments have been provided by T. Damour and K. Nordtvedt. We benefited from conversations with J. D. Anderson and R. W. Hellings. We wish to acknowledge and thank the staffs of CERGA, Haleakala, the University of Texas McDonald Observatory, and the Lunar Laser Ranging associates. Normal points were constructed from individual photon returns by R. Ricklefs, P. Shelus, A. Whipple, and J. G. Ries at the University of Texas for the MLRS and for earlier Haleakala data. D. O'G: a produced later Haleakala normal points. C. Veillet provided normal points for the CERGA data. The planetary ephemeris was produced by E. M. Standish. The research described in this paper was carried out at the Jet Propulsion Laboratory, California Institute of Technology, under a contract with the National Aeronautics and Space Administration.

- 
- [1] J. O. Dickey *et al.*, *Science* **265**, 482 (1994).  
 [2] J. G. Williams *et al.*, *Phys. Rev. Lett.* **36**, 551 (1976).  
 [3] I. I. Shapiro, C. C. Counselman, and R. W. King, *Phys. Rev. Lett.* **36**, 555 (1976).  
 [4] I. I. Shapiro *et al.*, *Phys. Rev. Lett.* **61**, 2643 (1988).  
 [5] J. O. Dickey, X. X. Newhall, and J. G. Williams, *Adv. Space Res.* **9**, 75 (1989).  
 [6] T. D. Moyer, *Celest. Mech.* **23**, 33 (1981).  
 [7] C. M. Will, in *Experimental Gravitation*, edited by B. Bertotti (Academic, New York, 1974), p. 1.  
 [8] X. X. Newhall, E. M. Standish, and J. G. Williams, *Astron. Astrophys.* **125**, 150 (1983).  
 [9] I. I. Shapiro, *Phys. Rev. Lett.* **13**, 789 (1964).  
 [10] D. B. Holdridge, in *Supporting Research and Advanced Development, Space Programs Summary 37-48*, Jet Propulsion Laboratory report, 1967 (unpublished), Vol. III, pp. 2-4.  
 [11] T. D. Moyer, JPL Internal Memorandum No. 314.7-122, 1977 (unpublished).  
 [12] E. M. Standish, *Astron. Astrophys.* **233**, 252 (1990).  
 [13] K. Nordtvedt, Jr., *Phys. Rev.* **169**, 1014 (1968); **169**, 1017 (1968); **170**, 1186 (1968).  
 [14] K. Nordtvedt, Jr., *Phys. Rev. D* **43**, 3131 (1991).  
 [15] K. Nordtvedt, Jr., *Icarus* **114**, 51 (1995).  
 [16] T. Damour and D. Vokrouhlický, *Phys. Rev. D* **53**, 4177 (1996).  
 [17] F. M. Flasar and F. Birch, *J. Geophys. Res.* **78**, 6101 (1973).  
 [18] E. G. Adelberger *et al.*, *Nature (London)* **347**, 261-263 (1990).  
 [19] G. Smith (private communication).  
 [20] M. Chapront-Touzé and J. Chapront, *Astron. Astrophys.* **190**, 342 (1988); M. Chapront-Touzé and J. Chapront, *Lunar Tables and Programs from 4000 B.C. to A.D. 8000* (Willman-Bell, Richmond, VA, 1991).  
 [21] V. A. Brumberg and T. V. Ivanova, in *Sun and Planetary Systems*, edited by W. Fricke and G. Teleki (Reidel, Dordrecht, 1982), p. 423.  
 [22] V. A. Brumberg and T. V. Ivanova, *Bull. Inst. Theor. Astron.* **19**, 3 (1985).  
 [23] J.-F. Lestrade and M. Chapront-Touzé, *Astron. Astrophys.* **116**, 75 (1982).  
 [24] K. Nordtvedt, Jr., *Phys. Rev. D* **37**, 1070 (1988).  
 [25] B. Shahid-Saless, *Phys. Rev. D* **46**, 5404 (1992).  
 [26] K. Nordtvedt, Jr., *Phys. Rev. D* **47**, 3633 (1993).  
 [27] V. J. Slabinski (private communication).  
 [28] K. Nordtvedt, Jr., *Phys. Rev. D* **43**, 3131 (1991).  
 [29] E. G. Adelberger *et al.*, *Phys. Rev. D* **42**, 3267 (1990).  
 [30] P. G. Roll, R. Krotkov, and R. H. Dicke, *Ann. Phys. (N.Y.)* **26**, 442 (1964).  
 [31] V. B. Braginsky and V. I. Panov, *Zh. Eksp. Teor. Fiz.* **61**, 873 (1971) [*Sov. Phys. JETP* **34**, 463 (1972)].  
 [32] Y. Su *et al.*, *Phys. Rev. D* **50**, 3614 (1994).  
 [33] R. D. Reasenber *et al.*, *Astrophys. J. Lett.* **234**, L219 (1979).  
 [34] J. Müller *et al.*, *Astrophys. J.* **382**, L101 (1991). The Earth-Moon orbit about the Sun contributes uncertainty which was not considered in the solutions, and the uncertainties given in the following two references are more realistic [J. Müller (private communication)]: J. Müller *et al.*, in *Proceedings of the*

- Second Gauss Symposium, Munich, Germany, 1993 (unpublished); J. Müller *et al.*, in *General Relativity, Proceedings of the Seventh Marcel Grossman Meeting*, Stanford, California, 1994, edited by R. Reygini and M. Keiser (World Scientific, Singapore, 1995).
- [35] A. J. Ferrari *et al.*, *J. Geophys. Res.* **85**, 3939 (1980).
- [36] I. I. Shapiro, in *Proceedings of the 12th International Conference on General Relativity and Gravitation*, University of Colorado at Boulder, 1989, edited by N. Ashby, D. Bartlett, and W. Wyss (Cambridge University Press, Cambridge, England, 1990), p. 313.
- [37] J. F. Chandler, R. D. Reasenberg, and I. I. Shapiro, *Bull. Am. Astron. Soc.* **26**, 1019 (1994).
- [38] W. de Sitter and D. Brouwer, *Bull. Astron. Inst. Neth.* **8**, 213 (1938).
- [39] B. M. Barker and R. F. O'Connell, *Phys. Rev. D* **2**, 1428 (1970); **12**, 329 (1975).
- [40] B. Bertotti, I. Ciufolini, and P. L. Bender, *Phys. Rev. Lett.* **58**, 1062 (1987).
- [41] J. G. Williams, W. S. Sinclair, and C. F. Yoder, *Geophys. Res. Lett.* **5**, 943 (1978).
- [42] A. S. Konopliv *et al.*, in *Proceedings of the AAS/AIAA Astrodynamics Conference*, Victoria, BC, 1993, edited by A. K. Misra, V. J. Modi, R. Holdaway, and P. M. Bainam (Univelt, San Diego, CA, 1993), pp. 1275–1294.
- [43] M. T. Zuber *et al.*, *Science* **266**, 1839 (1994); F. G. Lemoine, D. E. Smith, and M. T. Zuber, *Eos* **75**, 400 (1994).
- [44] J. G. Williams, X. X. Newhall, and J. O. Dickey, *Planet. Space Sci.* (to be published).
- [45] K. Nordtvedt, Jr. (private communication).
- [46] I. I. Shapiro *et al.*, *J. Geophys. Res.* **82**, 4329 (1977).
- [47] D. L. Cain *et al.*, *Bull. Am. Astron. Soc.* **10**, 387 (1978).
- [48] R. W. Hellings, in *Proceedings of the 10th International Conference on Relativity and Gravitation*, Padova, edited by B. Bertotti *et al.* (Reidel, Dordrecht, 1983), pp. 365–385.
- [49] M. H. Soffel, *Relativity in Astrometry, Celestial Mechanics, and Geodesy* (Springer-Verlag, Berlin, 1989).
- [50] C. F. Yoder, *Philos. Trans. R. Soc. London A* **303**, 327 (1981).
- [51] R. W. Hellings *et al.*, *Phys. Rev. Lett.* **51**, 1609 (1983).
- [52] J. D. Anderson *et al.*, in *Sixth Marcel Grossman Meeting*, Proceedings, Kyoto, Japan, 1991, edited by H. Sato and T. Nakamura (World Scientific, Singapore, 1992), p. 353.
- [53] E. V. Pitjeva, *Celest. Mech. Dyn. Astron.* **55**, 313 (1993).
- [54] J. F. Chandler, R. D. Reasenberg, and I. I. Shapiro, *Bull. Am. Astron. Soc.* **25**, 1233 (1993).
- [55] T. Damour *et al.*, *Phys. Rev. Lett.* **61**, 1151 (1988).
- [56] J. H. Taylor and J. M. Weisberg, *Astrophys. J.* **345**, 434 (1989).
- [57] J. H. Taylor, in *Particle Astrophysics*, Fourth Rencontres de Blois, edited by J. Tran Thanh Vân (Editions Frontieres, Gif-sur-Yvette, 1993), p. 367.
- [58] V. M. Kaspi, J. H. Taylor, and M. F. Ryba, *Astrophys. J.* **428**, 713 (1994).